Numerical Simulation of Remagnetization Processes in Extended Thin Films and Periodic Nanodot Arrays

Dmitri V. BERKOV*, Natalia L. GORN

***Abstract*--The best approach to compute the long-range stray field by micromagnetic simulations of systems with periodic boundary conditions (PBC) on regular grids is the FFT-based solution of the Poisson equation combined with the Ewald method to ensure a rapid convergence of the Fourier series. Here we present the version of such a FFT-Ewald method suitable for grids of rectangular cells. Further, we have incorporated the evaluation of the near-field part of the Ewald sums into the FFT-procedure used to evaluate the field of the Gaussian dipole lattice, so that no additional time is spent for the near-field computation. The method described can be used for simulation of any 3D or 2D systems with PBC. We present physical examples dealing with extended thin films and arrays of nanowires and nanodots.**

***Index Terms*—magnetic nanodots, magnetic thin films, magnetodipolar interaction, periodic boundary conditions.**

I. Introduction

One of the major problems by simulating magnetic systems with periodic boundary conditions (PBC) is the computation of the long-range dipolar interaction (stray) field $\mathbf{H}_{\text{dip}}$. Various methods have been suggested for the solution of this problem: summation over several nearest neighbour shells using some cut-off [1], hierarchical summation [2], direct solution of a Poisson equation for the scalar magnetic potential of a dipole lattice [3], extended Lorentz cavity method [4] etc. Among them the Ewald method [5] combined with the FFT-based solution of the Poisson equation is in principle the best choice. Its advantages are [6]: (i) high speed (~$N\cdot\log N$ – algorithm), (ii) ability to handle 2D and 3D systems, (iii) correct treatment of the dipolar interaction for macroscopically non-homogeneous magnetization patterns and (iv) absence of artificial field oscillations in case of abrupt magnetization changes.

In [6] we have described the FFT-Ewald method for stray field calculations in systems of *point* or *spherical* dipoles. This approximation provides satisfactory results also for systems of rectangular finite elements (cells) with sizes approximately equal in all three dimensions. However, it clearly fails if the cell size in one direction should be much larger or smaller than in another directions (as, e.g., for thin or relatively thick films). In this paper we report the generalization of the point-dipole FFT-Ewald method described in [6] to lattices of rectangular cells with arbitrary sides and present physical examples where the application of this method is necessary.

* Manuscript received Feb. 04, 2002.

The author is with *INNOVENT* e.V. Technology, D-07745, Jena, Germany (e-mail: db@innovent-jena.de).

Digital Object Identifier DOI: 10.1109/TMAG.2002.803618

II. Ewald Method for Rectangular Prismatic Dipoles

To construct the Ewald method version for the lattice of rectangular prismatic cells (with the sides Δ_x, Δ_y and Δ_z and volumes $V_c = \Delta_x\Delta_y\Delta_z$) each carrying the dipole moment $\mathbf{m}_{ij}^{\text{rect}}$ we proceed as usual. First, we *add* and *subtract* to each lattice cell the Gaussian dipole with the magnetization density

$$\mathbf{m}_{ij}^{\text{G}}(\mathbf{r}) = -\frac{V_c}{(2\pi)^{3/2} a_{\parallel}^2 a_{\perp}} \cdot \sum_{\gamma} m_{ij}^{\gamma} \mathbf{e}_{\gamma} \cdot e^{-\frac{x^2+z^2}{2a_{\parallel}^2} - \frac{y^2}{2a_{\perp}^2}} \tag{1}$$

($\gamma = x,y,z$). It has the same total moment as the original rectangular dipole and opposite direction. The stray field of the resulting system can be calculated as the sum of the fields of (i) the lattice of Gaussian dipoles (1) with the magnetization

$$\mathbf{m}^{\text{GL}}(\mathbf{r}) = \sum_{i,j} \mathbf{m}_{ij}^{\text{G}}\left(\mathbf{r} - \mathbf{r}_{ij}\right) \tag{2}$$

and (ii) the lattice where the rectangular dipole on each site is compensated by the negative Gaussian dipole

$$\mathbf{m}^{\text{sr}}(\mathbf{r}) = \sum_{i,j}\left[\mathbf{m}_{ij}^{\text{rect}}\left(\mathbf{r} - \mathbf{r}_{ij}\right) - \mathbf{m}_{ij}^{\text{G}}\left(\mathbf{r} - \mathbf{r}_{ij}\right)\right] \tag{3}$$

A. Field of the Lattice of 3d Gaussian Dipoles

We calculate the field of the Gaussian lattice (2) by solving the Poisson equation for the magnetic scalar potential $\Delta\phi(\mathbf{r}) = -4\pi\rho(\mathbf{r})$ where the 'magnetic charge' density is defined as $\rho(\mathbf{r}) = -\text{div}(\mathbf{m}(\mathbf{r}))$. The procedure is fully analogous to that described in [6], except that we have to *average* the resulting field over the volume of the cell on which we calculate the field.

Keeping in mind the application of the method to magnetic multilayers, we introduce the coordinate system with 0x and 0z axis in the layer plane and 0y axis perpendicular to it. In this coordinates, the *in-plane* components of the stray field from the source layer (#1) on the target layer (#2) can be written as

$$H_{1\to 2}^{x(z)}\left(\mathbf{r}_{ij}, d_{12}\right) = -C_N \cdot \sum_{\{\mathbf{k}_{\parallel}\}} F\left(\mathbf{k}_{\parallel}, \mathbf{r}_{ij}\right) \cdot k_{z(x)}^{-1} \cdot \left\{\left[k_x m_x(\mathbf{k}_{\parallel}) + k_z m_z(\mathbf{k}_{\parallel})\right] \cdot I_{-1} + i \cdot m_y(\mathbf{k}_{\parallel}) \cdot J\right\} \tag{4}$$

and the *perpendicular* stray field projection is

$$H^{y}_{1\to 2}\left(\mathbf{r}_{ij}, d_{12}\right) = -C_N \cdot \sum\nolimits_{\{\mathbf{k}_{\|}\}} F\left(\mathbf{k}_{\|}, \mathbf{r}_{ij}\right) \cdot k_x^{-1} k_z^{-1} \cdot \left\{ i \cdot \left[k_x m_x(\mathbf{k}_{\|}) + k_z m_z(\mathbf{k}_{\|}) \right] \cdot J + m_y(\mathbf{k}_{\|}) \cdot I_1 \right\} \quad (5)$$

The normalizing constant C_N depends on the discretization cell numbers N_x and N_z in lateral (in-plane) directions and the in-plane cell sizes Δ_x and Δ_z (which should be the same for all layers) and layer thicknesses $\Delta_y^{(1,2)}$ (which may be different):

$$C_N = \frac{16}{N_x N_z} \cdot \frac{\Delta_y^{(1)}}{\Delta_y^{(2)}} \cdot \frac{1}{\Delta_x \Delta_z}$$

The function F present in both expressions (4) and (5)

$$F\left(\mathbf{k}_{\|}, \mathbf{r}_{ij}\right) = e^{ik_{\|} r_{ij} - \frac{1}{2} k_{\|}^2 a_{\|}^2} \cdot \sin\left(k_x \Delta_x / 2\right) \cdot \sin\left(k_z \Delta_z / 2\right)$$

shows that the Fourier components of the Gaussian lattice field decay exponentially with the in-plane wave vector magnitude $k_{\|}$. This fact ensures the absence of the artificial field oscillations due to the unavoidable cut-off of the spectrum on the largest spatial frequency available for the given discretization.

The fields (4) and (5) include integrals

$$J\left(k_{\|}, d_{12}\right) = 2 \int_0^{\infty} \frac{e^{-\frac{k_{\perp}^2 a_{\perp}^2}{2}}}{k_{\perp}^2 + k_{\|}^2} \sin\left(k_{\perp} \Delta_y^{(2)} / 2\right) \sin\left(k_{\perp} d_{12}\right) dk_{\perp}$$

$$I_p\left(k_{\|}, d_{12}\right) = 2 \int_0^{\infty} \frac{k_{\perp}^p e^{-\frac{k_{\perp}^2 a_{\perp}^2}{2}}}{k_{\perp}^2 + k_{\|}^2} \sin\left(k_{\perp} \Delta_y^{(2)} / 2\right) \cos\left(k_{\perp} d_{12}\right) dk_{\perp}$$

which result from the Fourier integral expansion of the Poisson equation in the direction perpendicular to the layer plane (in which the system is *not* translationally invariant).

B. Evaluation of the short-range contribution

The field created by the compensated dipoles ($\mathbf{m}_{ij}^{\text{rect}}$-$\mathbf{m}_{ij}^{\text{G}}$) of the lattice (3) is the short range one, because the original rectangular dipole is completely screened by the negative Gaussian dipole on the distances $r \gg \max(a_{\|}, a_{\perp})$. Thus it is sufficient to calculate this contribution from each cell on its several nearest neighbours only [5, 6].

The straightforward computation of this short-range field can be reduced to the calculation of the so called Ewald coefficients, which in our case represent the difference between the fields created by a unit rectangular dipole directed along one of the coordinate axes and a corresponding negative Gaussian dipole. This difference should be averaged over the volume of the target cell. This operations amount to numerical evaluation of four-fold integrals, which is an unstable and time-consuming procedure (even taking into account that it has to be performed only once). For this reason we have developed the fast and reliable method to evaluate Ewald coefficients from (i) the *analytically* known interaction energy of rectangular prisms (tabulated in, e.g., [7]) and (ii) a field created by one Gaussian dipole placed on a lattice with PBC, which can be computed numerically using the expressions (4-5). Evaluating this latter field for various lattice sizes and extrapolating it towards the infinite size, we obtain a required field of a *single* Gaussian dipole. Details of this procedure will be described elsewhere.

Further advantage of our FFT-Ewald version results from the fact, that the short-range contribution also depends on the distance between the source and target cells only. Thus we could incorporate the Ewald coefficients into the FFT-procedure originally used to evaluate the contribution of the Gaussian dipole lattice (4-5), so that *no additional time* is spent for the near-field computation at all.

III. Physical Examples

PBC are used to avoid finite-size effects but nevertheless to take into account properly all relevant magnetic interactions. Three wide-spread cases when PBC are for these reasons unavoidable, are: (i) extended thin films, (ii) so called magnetic nanowires (thin long stripes with the width in the sub-μm-region) and (ii) periodic arrays of thin film elements with both lateral sizes in the same region, called nanodots.

In all examples below the quasistatic remagnetization processes were simulated using a strongly optimized version of a Modified Steepest Descent and Relaxation (MSDR) algorithm [8]. We have started from a large saturating field and used the equilibrium configuration obtained in the previous field as a starting state for the next one. The 0*xz*-plane of the coordinate system always lies in the film plane; 0*x*-axis is aligned horizontally relative to the gray-scale images shown in Fig. 1-3.

A. Remagnetization of an Extended Film

As an example we show here the remagnetization curve of a thin (thickness h = 10 nm) polycrystalline film with the average crystallite size D = 20 nm, 'made' of a magnetically hard material like Co (exchange stiffness $A = 10^{-6}$ erg/cm, saturation magnetization M_S = 1000 G, uniaxial anisotropy of a single grain $K_u = 4 \cdot 10^6$ erg/cm^3, randomly (in 3d) distributed grain anisotropy axes). Full exchange across the intergrain boundaries was assumed.

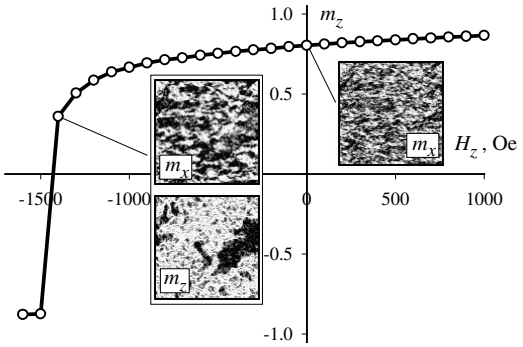

Fig. 1. Remagnetization curve and gray scale maps of the magnetization projections of a polycrystalline extended thin film made of 'hard' magnetic material. Size of the images shown is 2 x 2 μm. See text for details.

Simulation of a quasistatic remagnetization process of this film were performed using a N_x x N_z = 400 x 400 discretization of a 2 x 2 μm area. Results presented in Fig. 1 demonstrate, as

expected, that remagnetization in such a 'hard' film starts from the reversal of a single grain(s) which due to the fluctuation of the polycrystalline structure has the smallest switching field. Afterwards this reversed grain serves as a nucleus for the entire film remagnetization, assisting the reversal of neighbouring grains via the strong intergrain exchange. This mechanism is also responsible for very different correlation lengths of m_x- and m_z- projections (compare corresponding images in Fig. 1).

B. Remagnetization of an Array of Nanowires

We have studied remagnetization of thin (h=10 nm) polycrystalline (D = 20 nm) stripes with a width w = 500 nm and magnetic parameters as for Py in a field directed along the stripes. Simulations of a 4 x 4 μm area discretized into 400 x 400 cells were performed.

The remagnetization of long magnetic elements with such a small thickness occurs via the formation of 360° domain walls, as explained in [9]. Our results (Fig. 2) are consistent with this observation. The overall character of the remagnetization process strongly depends on the distance between stripes due to the dipolar interaction effects: For well separated wires (distance between stripes w_{sep} = 500 nm) remagnetization patterns of different stripes are uncorrelated - see gray-scale magnetization maps on the left in Fig. 2 - leading to a relatively broad hysteresis (solid line in Fig. 2). For closely placed wires (w_{sep} = 40 nm, dash-dotted line) a cooperative switching occurs, as it can be clearly seen from m_x and m_z gray scale-maps presented in the same figure on the right. We note that in our case 360° domain walls are additionally stabilized by the strong demagnetizing effects due to the perfect stripe borders assumed in these simulations.

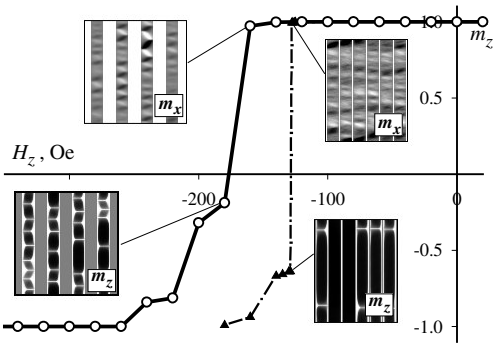

Fig. 2. Remagnetization of an array of separated (solid line with open circles) and closely placed (dash-dotted line with triangles) 'soft' magnetic stripes (thickness h = 10 nm, stripe width w = 500 nm). Note the cooperative switching in the latter case.

C. Nanodot Arrays

Simulations of the remagnetization processes in periodic systems of Py magnetic nanodots we have performed also for arrays of closely packed and separated elements - circular nanodots h = 10 nm thick and d = 500 nm in diameter. Results for the same simulation area and discretization as for nanowires are shown in Fig. 3. Separated nanodots (interdot distance w_{sep} = 250 nm) again show uncorrelated magnetization patterns (images on the left of Fig. 3). Corresponding remagnetization curve (solid line) is in a reasonable qualitative agreement with hysteresis loops measured on similar systems in, e.g., [10].

The remagnetization of closely packed nanodots occurs in a completely different - and highly correlated - way due to the dipolar interaction effects (Fig. 3, dash-dotted line, m_x-gray-scale maps on the right). In this case such a collective behaviour results in a *higher* coercivity, but *lower* negative saturation field than for independent nanodots.

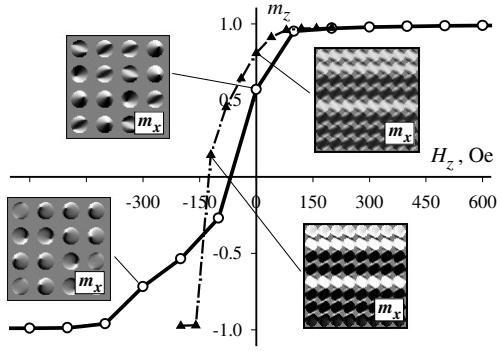

Fig. 3. Remagnetization of an array of well separated (solid line, open circles) and closely placed (dash-dotted line, filled triangles) nanodots (thickness h = 10 nm, diameter d = 500 nm) made of a 'soft' magnetic material. Again, the switching for a closely packed system is highly cooperative.

ACKNOWLEDGMENT

The authors would like to thank Dr. R. Mattheis for useful discussions and Prof. P. Görnert for continuous support.

REFERENCES

[1] J.-G. Zhu, H.N. Bertram, "Micromagnetic studies of thin metallic films", *J.Appl.Phys.*, vol. 63, pp. 3246-3253, 1988

[2] J.J. Miles, B.K. Middleton, „A hierarchical micromagnetic model of longitudinal thin film recording media", *J. Magn. Magn. Mat*., vol. 95, pp. 99-108, 1991.

[3] R.C. Giles, P.R. Kotiuga, M. Mansuripur, „Parallel micromagnetic simulations using Fourier methods on a regular hexagonal lattice", *IEEE Trans. Magn.*, vol. MAG-27, pp. 3815-3817, 1991

[4] M.J. Vos, R.L. Brott, J. Zhu, L.W. Carlson, "Computed hysteresis behavior and interaction effects in spheroidal particle assemblies", *IEEE Trans. Magn*., vol. MAG-29, pp. 3652-3654, 1993

[5] K. De'Bell, A.B. MacIsaac, J.P. Whitehead, "Dipolar effects in magnetic thin films and quasi-two-dimensional systems", *Rev. Mod. Phys*., vol. 72, pp. 225-257, 2000

[6] D.V.Berkov, N.L.Gorn, "Quasistatic remagnetization processes in 2D systems with random on-site anisotropy and dipolar interaction: numerical simulations", *Phys.Rev*., vol. B57, pp. 14332-14343, 1998

[7] K. Ramstöck, T. Leibl, A. Hubert, "Optimizing stray field computations in finite-element micromagnetics", *J. Magn. Magn. Mat*., vol. 135, pp. 97-110, 1994

[8] K. Ramstöck, "Mikromagnetische Rechnungen an isolierten und eingebetteten Strukturen", PhD Thesis (in German), Univ. of Erlangen, Germany

[9] A. Hubert, R. Schäfer, *Magnetic domains: the analysis of magnetic microstructures*, Springer-Verlag, 1998 (pp. 472-473)

[10] M. Schneider, H. Hoffmann, "Magnetization loops of submicron ferromagnetic permalloy dot ararys", *J. Appl. Phys*., vol. 86, pp. 4539-4543, 1999